Contingency Assessment and Network Reconfiguration in Distribution Grids Including Wind Power and Energy Storage

Pilar Meneses de Quevedo, Javier Contreras, *Fellow, IEEE*, Marcos J. Rider, *Member, IEEE*, and Javad Allahdadian

***Abstract*—In case of abnormal conditions, distribution systems should be reconfigured to overcome the impacts of outages such as overloads of network components and increased power losses. For this purpose, energy storage systems (ESS) and renewable energy sources (RES) can be applied to improve operating conditions. An optimal contingency assessment model using two-stage stochastic linear programming including wind power generation and a generic ESS is presented. The optimization model is applied to find the best radial topology by determining the best switching sequence to solve contingencies. The proposed model is applied to a 69-node distribution system and the results of all possible contingencies in the network are examined considering three different case studies with several scenarios. In addition, a reconfiguration analysis including all the contingencies is presented for the case studies.**

***Index Terms*—Contingency analysis (CA), distributed generation (DG), islanding, optimal power flow, stochastic programming, storage devices.**

NOTATION

Indexes:

i, j, k	Node index.
r	Block index of linearization.
t	Real-time period index on a 10-min basis.
ω	Scenario index.

Parameters:

C^{sw}	Switching cost (\$).
C^{loss}	Real power losses cost (\$/MWh).
C^{w_curt}	Wind curtailment cost (\$/MWh).
C^{d_curt}	Real power demand curtailment cost (\$/MWh).
C^{sub}	Cost of real power from substation (\$/MWh).
C^{sp}	Production scheduled cost (\$/MWh).
C^{ss}	Storage scheduled cost (\$/MWh).
C^{rp}	Production scheduled reserve cost (\$/MWh).
C^{rs}	Storage scheduled reserve cost (\$/MWh).
$\hat{C}^{\text{rs}}$	Real-time energy storage cost (\$/MWh).
$\hat{C}^{\text{rp}}$	Real-time energy production cost (\$/MWh).
C_{ij}	State of a contingency in branch *ij*.
$d_{it\omega}$	Real power demand at node i (MW).
$q_{it\omega}$	Reactive power demand at node i (MVAr).
ini_{ij}	Initial state of a switch in branch *ij*.
$\overline{I}_{ij}$	Maximum current flow in branch *ij* (A).
$m_{ijrt\omega}$	Slope of the rth block for branch *ij*.
N_{loop}	Number of switches in a loop.
PF_i	Power factor (PF) of the load at node i.
$P^{\text{fore}}_{it\omega}$	Wind real power forecast at node i (MW).
R^{tot}	Total number of blocks in the piecewise linearization.
$\underline{s}^s_i, \overline{s}^s_i$	Minimum/maximum power storage at node I (MW).
$\underline{s}^p_i, \overline{s}^p_i$	Minimum/maximum production at node i (MW).
R_{ij}	Resistance of branch *ij* (Ω).
X_{ij}	Reactance of branch *ij* (Ω).
Z_{ij}	Impedance of branch *ij* (Ω).
V_{nom}	Nominal voltage of the distribution network (kV).
$\underline{V}_i, \overline{V}_i$	Minimum/maximum voltage at node i (kV).
$\overline{W}$	Upper bound of variable $W_{ijt\omega}$ (kV).
x^s_{i0}	Initial energy level of storage unit at node i (MWh).
$\underline{x}_i, \overline{x}_i$	Min/max storage capacity at node i (MWh).
η^s_i, η^p_i	Efficiency storage/production rates.
$\Delta S_{ijrt\omega}$	Upper bound for the rth block of the power flow through branch *ij*.
Δ	Real-time period (10 min) (h).

Nonnegative variables:

$I^2_{ijt\omega}$	Square of the current flow of branch *ij* (A^2).
$P^{\text{wind}}_{it\omega}$	Real power wind generation at node i (MW).
$P^{w\_\text{curt}}_{it\omega}$	Real power wind curtailment at node i (MW).
$P^{d_{\text{curt}}}_{it\omega}$	Real power demand curtailment at node i (MW).
$P^2_{ijt\omega}$	Square of the real power in branch *ij* (MW^2).
$Q^2_{ijt\omega}$	Square of the reactive power in branch *ij* (MVAr^2).
$P^+_{ijt\omega}$	Real power flow in branch *ij*, downstream (MW).
$P^-_{ijt\omega}$	Real power flow in branch *ij*, upstream (MW).
$Q^+_{ijt\omega}$	Reactive power flow (downstream) (MVAr).
$Q^-_{ijt\omega}$	Reactive power flow (upstream) (MVAr).
r^p_i, r^s_i	Scheduled power production/storage reserve (MW).

Manuscript received February 23, 2015; revised May 19, 2015; accepted July 05, 2015. This work was supported in part by the European Union 7th Framework Programme under Grant 309048, project SiNGULAR, and in part by the Ministry of Science of Spain under CICYT Project ENE2012-30679. Paper no. TSTE-00134-2015.

P. Meneses de Quevedo and J. Contreras are with E.T.S. de Ingenieros Industriales, University of Castilla–La Mancha, 13071 Ciudad Real, Spain (e-mail: pilar.meneses@uclm.es; javier.contreras@uclm.es).

M. J. Rider is with the Department of Systems and Energy, University of Campinas, 13083-852 Campinas, Brazil (e-mail: mjrider@dsee.fee.unicamp.br).

J. Allahdadian is with the Department of Energy (DENERG), Politecnico di Torino, 10129 Turin, Italy (e-mail: javad.allahdadian@polito.it).

Color versions of one or more of the figures in this paper are available online at http://ieeexplore.ieee.org.

Digital Object Identifier 10.1109/TSTE.2015.2453368

$\hat{r}^p_{it\omega}$, $\hat{r}^s_{it\omega}$ Real-time production/storage reserve (MW).
s^p_i, s^s_i Scheduled power production/storage (MW).
$V^2_{it\omega}$ Square of the voltage magnitude at node i (kV^2).
$W^2_{ijt\omega}$ Square of the voltage drop for branch *ij* (kV^2).
$\hat{x}_{it\omega}$ Storage level at node i (MWh).
$\Delta P_{ijrt\omega}$ Value of the rth block of real power (MW).
$\Delta Q_{ijrt\omega}$ Value of the rth block of reactive power (MVAr).

Free variables:
$P^{\text{sub}}_{it\omega}$ Real power of a substation at node i (MW).
$Q^{\text{sub}}_{it\omega}$ Reactive power of a substation at node i (MVAr).
$Q^{\text{wind}}_{it\omega}$ Reactive power of wind generation at node i (MVAr).
$Q^{d_{\text{curt}}}_{it\omega}$ Demand reactive power curtailment (MVAr).

Binary variables:
$v^{P+}_{ijt\omega}$ Variable related to real power (upstream).
$v^{P-}_{ijt\omega}$ Variable related to real power (downstream).
$v^{Q+}_{ijt\omega}$ Variable related to reactive power (upstream).
$v^{Q-}_{ijt\omega}$ Variable related to reactive power (downstream).
v^s_{it}, v^p_{it} Variables related to storage or production.
y_{ij} State of the switch in branch *ij*.

I. Introduction

CONTINGENCY analysis (CA) provides tools to study contingencies in electrical networks and analyze their behavior in case of outages in one of the electrical components such as lines, transformers, and generators. Several studies have been carried out to assess contingencies in electrical networks. The comparison of some techniques such as ranking, screening, bounding, and fast power flow techniques has been done in [1] and [2]. Methods such as genetic algorithms [3], [4], bi-level programming [5], and other new power flow calculation approaches [6] have been developed to solve CA problems. Likewise, in terms of behavior assessment of power networks, some works have been presented to evaluate voltage security [7], [8], operation of transmission networks [9], [10], and optimal switching under $N-1$ contingencies [11]–[13].

Moreover, reconfiguration of distribution systems (RDS) aims at finding the best topology of the system concerning power losses, energy demand, and operational performance. In general, two major groups of optimization methods have been represented to solve the RDS problem: 1) exact techniques and 2) heuristic and metaheuristic techniques. In literature, exact techniques such as branch and bound are only used to solve relaxed models [14]–[18]. On the contrary, heuristic and metaheuristic methods such as ant colony [19], [20], genetic algorithms [21]–[23], and particle swarm optimization [24] have been applied for complete models.

In particular, RDS can be used to improve the operation of distribution systems in case of contingencies, considering renewable energy sources (RES) and energy storage systems (ESS) in electrical networks. Although the availability of RES and ESS can be seen as an opportunity to exploit available resources near loads and compensate energy demand, problems may arise due to the intermittency and uncertainty of RES [4], [25] and the integration of ESS into electrical distribution systems (EDS) [26], [27].

A mixed integer linear programming (MILP) reconfiguration model under an $N-1$ reliability criterion using stochastic programming considering wind energy and ESS in EDS is introduced. The steady-state operation of a radial EDS is complicated to model linearly; hence, an alternative current (ac) flow is approximated through linear expressions. The proposed model also includes switching operation, intermittent RES, and generic ESS. The analysis of $N-1$ contingencies is performed using a contingency parameter per branch to locate the fault in the branch.

Due to several technical reasons such as low cost operation, simplicity of analysis and coordination, and reduction of short circuit current, EDS must operate with a radial topology (even with a meshed structure). In addition, MILP is applied, in this paper, due to the following advantages: 1) the mathematical model is robust; 2) the computational behavior of a linear solver is more efficient than nonlinear solvers; and 3) using classical optimization techniques, convergence can be guaranteed.

The main contributions of this paper are as follows.

1) Regarding the methodology, a two-stage stochastic mathematical MILP for contingency response is introduced to consider the inconsistency and intermittency of the renewable power sources.
2) From a modeling perspective, a joint programming model of the optimal reconfiguration and contingency evaluation is presented here for a distribution system. However, in the literature, optimal switching under contingency conditions is reported only for transmission networks [11]–[13].
3) The benefits of combining RES with ESS in distribution networks, especially under contingencies and abnormal conditions, are analyzed.

Another relevant aspect of the presented optimization model is the minimization of the overall operation costs, including switching and demand and wind curtailment costs. Note that the problem formulation assumes that the overall investment costs have already been minimized in a previous planning phase where the best locations for wind and storage have been selected in advance.

This paper is organized as follows. Section II describes the mathematical formulation of generation and storage models. Section III defines the mathematical model as a stochastic MILP. The main results of the case studies considering contingencies and reconfigurations are shown in Section IV. Finally, conclusion is presented in Section V.

II. Storage Modeling

In modern power systems, storage devices have grown rapidly. ESSs are integrated into EDS to consider several purposes such as meeting real-time power demand, smoothing output power of RES, improving power system reliability,

and being economically efficient [28]. Thus, a generic storage system is modeled as follows:

$$\underline{s}_i^s \le s_i^s + r_i^s \le \overline{s}_i^s v_{it}^s \tag{1}$$

$$\underline{s}_i^p \le s_i^p + r_i^p \le \overline{s}_i^p v_{it}^p \tag{2}$$

$$0 \le \hat{r}_{it\omega}^p \le r_i^p \tag{3}$$

$$0 \le \hat{r}_{it\omega}^s \le r_i^s \tag{4}$$

$$\underline{x}_i \le \hat{x}_{it\omega} \le \overline{x}_i \tag{5}$$

$$\hat{x}_{it\omega} = \hat{x}_{it-1\omega} + \Delta\left[\eta_i^s s_i^s - \left(1/\eta_i^p\right) s_i^p\right] + \Delta\left[\eta_i^s \hat{r}_{it\omega}^s - \left(1/\eta_i^p\right) \hat{r}_{it\omega}^p\right] \tag{6}$$

$$\hat{x}_{it=0\omega} = x_0^s \tag{7}$$

$$v_{it}^p + v_{it}^s \le 1. \tag{8}$$

The minimum and maximum storage limits (charge) and productions (injection into the network) are defined in (1) and (2). It is worth noting that s_i^s and $s_i^p$are implemented in these equations to smooth the output power of the storage unit and r_i^s/r_i^p to guarantee that real-time power balance is within the storage capacity. In (3) and (4), the actual real-time reserves are confined to the maximum reserve bounds r_i^s/r_i^p. The upper and lower bounds of energy capacity in storage units are defined by (5). The ESS transition function is represented by (6). Equation (7) limits the remaining energy in the storage unit. Finally, in (8), binary variables v_{it}^p and v_{it}^s are defined and added to (1) and (2) to avoid producing and storing energy simultaneously.

III. Stochastic Formulation of Contingency Assessment and Network Reconfiguration

The following assumptions are defined to represent the simplified operation of EDS including switches, generation, and storage devices.

1) The load pattern in EDS is altered every 10 min.
2) EDS are balanced three-phase systems and can be represented by an equivalent single-phase circuit.
3) Storage energy losses are ignored.
4) Storage and production of energy occur at constant power in storage units during real-time periods (10 min).
5) The location of storage units has already been defined in the planning phase.
6) Wind turbines are located at nodes with high demand.
7) The maximum contingency duration is 1 h, considering wind scenarios, which is divided into 10-min periods (six periods).
8) Faults are considered in feeders and circuit breakers.
9) Islanded radial operation of the system is possible with distributed generation (DG) integration.

To distinguish the direction (sense) of the current and power flow (forward or backward), two positive separate variables are shown in Fig. 1.

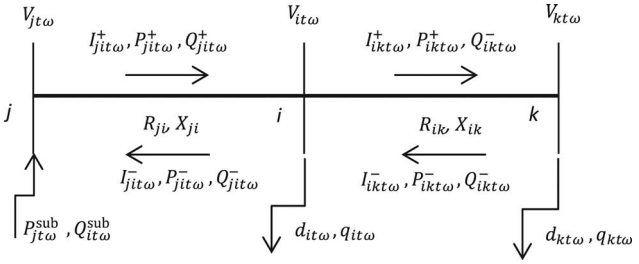

Fig. 1. Illustrative radial distribution system.

A. Objective Function

The objective function is formulated through two-stage stochastic programming as shown in (9)–(13). At the first stage, regardless of scenarios, i.e., only considering contingency conditions, the cost of opening and closing switches and the scheduling of storage units are assigned. At the second stage, the expected values of the total cost of power losses in the network, the cost of real-time production/storage of the storage units, and the cost of curtailment of both generation and demand, with respect to different scenarios and contingency conditions, are assigned. At the first stage, the variables are only related to contingency conditions and variables are relevant to both contingencies and scenarios at the second stage.

Objective function:

$$\min \phi + \gamma + E\left[\psi\left(\omega\right)\right] + E\left[K\left(\omega\right)\right] \tag{9}$$

where the first stage is given by $\phi + \gamma$:

1) Switching cost

$$\phi = \sum_{\substack{ij \\ \text{ini}_{ij}\,=\,0}} y_{ij} C^{\text{sw}} + \sum_{\substack{ij \\ \text{ini}_{ij}\,=\,1}} \left(1 - y_{ij}\right) C^{\text{sw}}. \tag{10}$$

2) Scheduled production/storage cost function

$$\gamma = \sum\nolimits_i \left[s_i^s C^{\text{ss}} + s_i^p C^{\text{sp}} + r_i^s C^{\text{rs}} + r_i^p C^{\text{rp}}\right]. \tag{11}$$

Next, the second stage is given by $\psi\left(\omega\right) + K\left(\omega\right)$:

1) Network costs (losses and substation costs)

$$\psi\left(\omega\right) = \Delta\left[\sum\nolimits_t \sum\nolimits_{ij} R_{ij} I_{ijt\omega}^2 C^{\text{loss}} + \sum\nolimits_t \sum\nolimits_i P_{it\omega}^{\text{sub}} C^{\text{sub}}\right]. \tag{12}$$

2) Corrective action costs (curtailment and real-time production/storage costs)

$$K\left(\omega\right) = \Delta\left[\sum\nolimits_t \sum\nolimits_i \left(P_{it\omega}^{w\_\text{curt}} C^{w\_\text{curt}} + P_{it\omega}^{d\_\text{curt}} C^{d\_\text{curt}} + \hat{r}_{it\omega}^p \hat{C}^{\text{rp}} + \hat{r}_{it\omega}^s \hat{C}^{\text{rs}}\right)\right]. \tag{13}$$

B. Constraints

The above objective function is subject to a set of constraints to assure optimal operational conditions.

1) Real-Time Power Balance Equations: Real power of wind including curtailment is represented in (14)

$$P_{it\omega}^{\text{wind}} = P_{it\omega}^{\text{fore}} - P_{it\omega}^{w_{\text{curt}}}. \tag{14}$$

Equations (15) and (16) represent the real and reactive power balances at node i, respectively (see Fig. 1). For both active and reactive power, wind power generation, scheduled production/storage, real-time production/storage power of ESS, the power flow from/to the substation, and power demand curtailment are considered. In addition, wind generation curtailment has already been formulated in (14)

$$\begin{aligned} P_{it\omega}^{\text{wind}} &+ \sum\nolimits_j \left(P_{jit\omega}^{+} - P_{jit\omega}^{-}\right) - \sum\nolimits_k \left[\left(P_{ikt\omega}^{+} - P_{ikt\omega}^{-}\right)\right. \\ &\left. + R_{ij} I_{ijt\omega}^2\right] + P_{it\omega}^{\text{sub}} + \left(\hat{r}_{it\omega}^{p} - \hat{r}_{it\omega}^{s}\right) + \left(s_i^p - s_i^s\right) \\ &= d_{it\omega} - P_{it\omega}^{d_{\text{curt}}} \end{aligned} \tag{15}$$

$$\begin{aligned} Q_{it\omega}^{\text{wind}} &+ \sum\nolimits_j \left(Q_{jit\omega}^{+} - Q_{jit\omega}^{-}\right) \\ &- \sum\nolimits_k \left[\left(Q_{ikt\omega}^{+} - Q_{ikt\omega}^{-}\right) + X_{ij} I_{ijt\omega}^2\right] + Q_{it\omega}^{\text{sub}} \\ &= q_{it\omega} - Q_{it\omega}^{d_{\text{curt}}}. \end{aligned} \tag{16}$$

2) Load PF: The following constraint is considered to keep the initial load PF:

$$Q_{it\omega}^{d_{\text{curt}}} = P_{it\omega}^{d_{\text{curt}}} * \left(\tan\left(\arccos\left(\text{PF}_i\right)\right)\right). \tag{17}$$

3) Voltage Drop Equations: The square value of the voltage drop between nodes is represented in (18) as an auxiliary variable $W_{ijt\omega}^2$, which is related to switching operations and contingencies

$$\begin{aligned} V_{it\omega}^2 &- 2\left(R_{ij}\left(P_{ijt\omega}^{+} - P_{ijt\omega}^{-}\right) + X_{ij}\left(Q_{ijt\omega}^{+} - Q_{ijt\omega}^{-}\right)\right) \\ &- Z_{ij}^2 I_{ijt\omega}^2 - V_{jt\omega}^2 + W_{ijt\omega}^2 = 0. \end{aligned} \tag{18}$$

The upper and lower bounds of the square of the voltage deviation for node i are defined by (19)

$$\underline{V}^2 \le V_{it\omega}^2 \le \overline{V}^2. \tag{19}$$

In constraints (20) and (21), $W_{ijt\omega}^2 = 0$ in case of operation of branch *ij* ($C_{ij} = 1$) or switch closure ($y_{ij} = 1$). To satisfy constraints (15) and (16), a proper value for parameter $\overline{W}^2$ should be set to give a sufficient degree of freedom for $W_{ijt\omega}^2$

$$W_{ijt\omega}^2 \ge -\bar{W}^2\left(1 - y_{ij}\right)\left(1 - C_{ij}\right) \tag{20}$$

$$W_{ijt\omega}^2 \le \bar{W}^2\left(1 - y_{ij}\right)\left(1 - C_{ij}\right) \tag{21}$$

4) Nonlinear Apparent Power Equation: The current flow magnitude calculation is represented by nonlinear constraint (22), where both sides of the constraint are linearized as explained in Section III-D

$$V_{jt\omega}^2 I_{ijt\omega}^2 = P_{ijt\omega}^2 + Q_{ijt\omega}^2. \tag{22}$$

5) Current and Power Magnitude Limits: Due to thermal limits in EDS, a set of constraints is introduced for current, real power, and reactive power in (23), (24)–(25), and (26)–(27), respectively. In addition, $v_{ijt\omega}^{P+}$, $v_{ijt\omega}^{P-}$, $v_{ijt\omega}^{Q+}$, and $v_{ijt\omega}^{Q-}$ are binary variables to avoid considering forward and backward power flows simultaneously. The constraints (23)–(27) define the limits through switching devices in branches if they are closed; otherwise, all magnitudes are equal to zero. Note that (24)–(27) are auxiliary constraints to improve the convergence of the proposed model

$$0 \le I_{ijt\omega}^2 \le \overline{I}_{ij}^2 C_{ij} y_{ij} \tag{23}$$

$$P_{ijt\omega}^{+} \le V_{\text{nom}} \overline{I}_{ij} v_{ijt\omega}^{P+} \tag{24}$$

$$P_{ijt\omega}^{-} \le V_{\text{nom}} \overline{I}_{ij} v_{ijt\omega}^{P-} \tag{25}$$

$$Q_{ijt\omega}^{+} \le V_{\text{nom}} \overline{I}_{ij} v_{ijt\omega}^{Q+} \tag{26}$$

$$Q_{ijt\omega}^{-} \le V_{\text{nom}} \overline{I}_{ij} v_{ijt\omega}^{Q-} \tag{27}$$

$$v_{ijt\omega}^{P+} + v_{ijt\omega}^{P-} \le y_{ij} \tag{28}$$

$$v_{ijt\omega}^{Q+} + v_{ijt\omega}^{Q-} \le y_{ij}. \tag{29}$$

C. Radial Configuration

The configuration of the network is radial by introducing constraint (30), i.e., the number of closed switches in any loop has to be less than the total number of switches in that loop. Therefore, by having at least one open branch in a loop, only a radial configuration of the network is feasible with the possibility of having one or more radial island(s) [29], [30]

$$\sum\nolimits_{ij} C_{ij} y_{ij} \le N_{\text{loop}} - 1. \tag{30}$$

Obviously, a branch between nodes i and j is disconnected in case of a contingency in that branch. Therefore, binary parameter C_{ij} is added to (30) to show that the branch is open in the mentioned case.

D. Linearization Procedure

The applied equations in the optimization problem are linear, excluding (22), which makes the model nonlinear. To cope with this problem, a linear approximation is proposed [31]. Both the left and right sides of (22) are nonlinear and both should be linearized separately. Note that $V_{jt\omega}^2$ and $I_{ijt\omega}^2$ are variables that represent the square magnitude values of voltages and currents, respectively, and they are used in (15)–(19), (22), and (23). In the following, the linearization process of (22) is described.

1) $V_{jt\omega}^2 I_{ijt\omega}^2$: The product of two variables is linearized by discretizing $V_{it\omega}^2$in small intervals. However, this leads to an increase in the number of binary variables and computation time. Since the voltage magnitude is within small range in EDS, a constant value V_{nom}^2 is selected and substituted for $V_{jt\omega}^2$ in (22) for the first iteration. Then, the model is run again and $V_{jt\omega}^2$ takes the value resulting from the first iteration. Note that $V_{jt\omega}^2$ hardly changes after the second iteration.

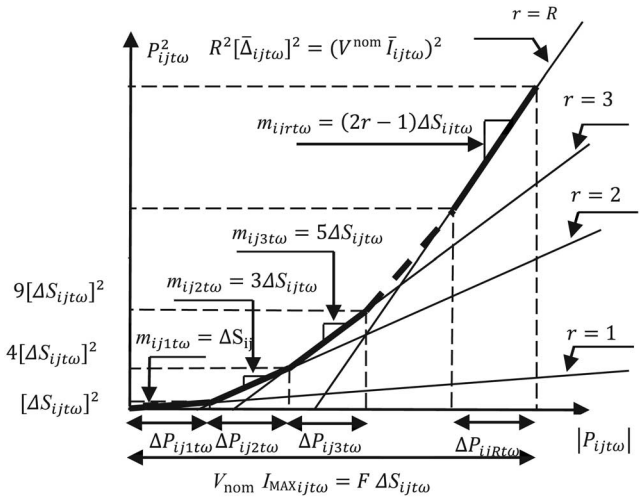

Fig. 2. Modeling the piecewise linear function $P^2_{ijt\omega}$.

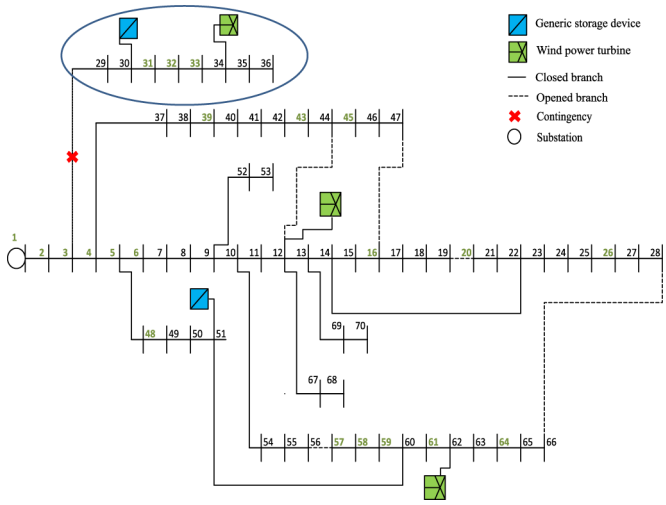

Fig. 3. 69-node network topology under a contingency in branch 3-29.

2) $P^2_{ijt\omega} + Q^2_{ijt\omega}$: The linearization of both terms on the right side of (22) is carried out by a piecewise linear approximation, as follows:

$$P^2_{ijt\omega} + Q^2_{ijt\omega} = \sum\nolimits_r (m_{ijrt\omega}\Delta P_{ijrt\omega}) + \sum\nolimits_r (m_{ijrt\omega}\Delta Q_{ijrt\omega}) \quad (31)$$

$$P^+_{jit\omega} + P^-_{jit\omega} = \sum\nolimits_r \Delta P_{ijrt\omega} \quad (32)$$

$$Q^+_{jit\omega} + Q^-_{jit\omega} = \sum\nolimits_r \Delta Q_{ijrt\omega} \quad (33)$$

$$0 \le \Delta P_{ijrt\omega} \le \Delta S_{ijrt\omega} \quad (34)$$

$$0 \le \Delta Q_{ijrt\omega} \le \Delta S_{ijrt\omega} \quad (35)$$

where

$$m_{ijrt\omega} = (2r-1)\,\Delta S_{ijrt\omega} \quad (36)$$

$$\Delta S_{ijrt\omega} = \left(V_{\text{nom}}\bar{I}_{ij}\right)/R^{\text{tot}} \quad (37)$$

Note that $m_{ijrt\omega}$ and $\Delta S_{ijrt\omega}$ are constant parameters and (32) and (33) are a set of linear expressions. Likewise, (31) is a linear approximation of $(P^2_{ijt\omega} + Q^2_{ijt\omega})$ and, (32) and (33) represent that $(P^+_{jit\omega} + P^-_{jit\omega})$ and $(Q^+_{jit\omega} + Q^-_{jit\omega})$ are equal to the sum of the values in each section of the discretization. As shown in (31)–(33) and Fig. 2, the right side of (22) can be replaced with the right side of (31) to form a linear equation

$$V^2_{\text{nom}} I^2_{ijt\omega} = \sum\nolimits_r (m_{ijrt\omega}\Delta P_{ijrt\omega}) + \sum\nolimits_r (m_{ijrt\omega}\Delta P_{ijrt\omega}). \quad (38)$$

The linear form of (22) is shown in (38). In this equation, V^2_{nom} is constant and $\sum_r (m_{ijrt\omega}\Delta P_{ijrt\omega})$ and $\sum_r (m_{ijrt\omega}\Delta Q_{ijrt\omega})$ are linear. The linearization of the active power flow is shown in Fig. 2.

IV. Case Studies

A. Network Overview

To evaluate the behavior of the proposed model, a 69-node network is considered and network data come from [32]. Fig. 3 depicts the 69-node network where the green nodes are not connected to loads and the locations of wind turbines and storage units are represented. The network is connected to a substation at node 1. The network contains 74 branches, 5 sectionalizing switches, and 5 tie-switches as shown in Table I, considering negligible opening and closing operation costs.

TABLE I
Switch Data for the 69-Node System

Sectionalizing switches			Tie switches		
12–44	14–22	16–47	7–8	19–20	31–32
28–66	51–60	–	41–42	56–57	–

TABLE II
Cost Data for 69-Node System ($/MWh)

C^{loss}	C^{w_curt}	C^{d_curt}	C^{ss}	C^{sp}	C^{rs}	C^{rp}	$\hat{C}^{\text{rs}}$	$\hat{C}^{\text{rp}}$
5	200	250	0.5	0.1	0.5	0.1	0.5	0.1

Other network costs are shown in Table II. The maximum current flow in the branches is 150 A, excluding branches L_{1-2} (line from nodes 1 to 2), L_{2-3}, and L_{3-4} with a maximum current limit of 100 A. Since the voltage values vary through iterations, the upper and lower voltage limits are defined as 1.1 and 0.9 p.u., respectively. In the linearization, 20 discrete blocks are considered. The total real power demand is 1.103 MW and the total time horizon is 1 h divided into 10 min periods. The demand data, recorded every 10 min, is collected from the Iberian Electricity Market [33], on March 20, 2014, and the contingency is assumed to occur at 4 A.M. Moreover, wind turbines are located at nodes 12, 34, and 62 with a production share of 16%, 34%, and 50%, respectively, and the total installed wind generation capacity is 0.45 MW. Two equal storage units are located at nodes 30 and 51, with a capacity of 0.15 MW allocated to each, and their initial energy levels are set to 50% of their capacities. The upper and lower limits of power storage/production in ESS are 0.075 MW.

B. Wind Production Scenarios

The exploitation of RES, especially wind, has had an upward trend leading to intermittency and uncertainty of power

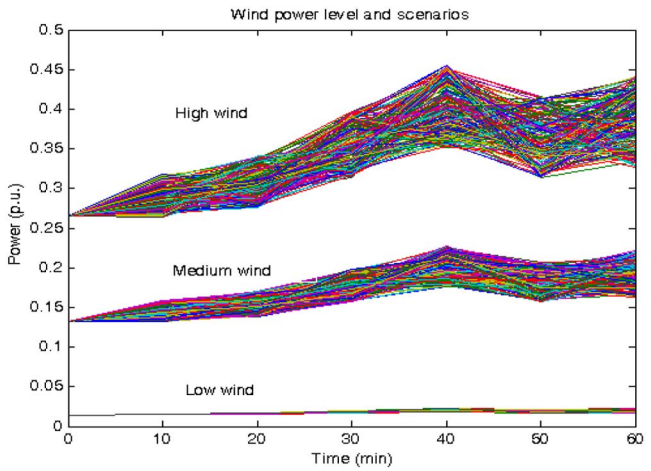

Fig. 4. Three different wind power point forecast and stochastic scenarios.

generation. In order to analyze the network under different conditions, three different stochastic levels of wind generation are introduced (low, mean, and high) as 1.5%, 16%, and 34% of the total demand. In this regard, to represent intermittency of wind power, 200 wind scenarios have been generated randomly by implementing Monte Carlo simulation under a cone of uncertainty, with the maximum error of 15% in 1 h for each forecast, as applied in [34] and [35]. The number of wind scenarios has been limited to 10 to minimize the dimensionality in the problem formulation maintaining accuracy in the results, by implementing a clustering mechanism, the K-means method, taking into account sequences of wind values every 10 min (six values) per scenario. This method can be used to partition a given set of scenarios into a given number of clusters. As a result of this partition, scenarios with similar features are assigned to the same cluster. The centroid of each cluster represents a somewhat average pattern of all the scenarios included in a cluster. Since this centroid is artificial, the original scenario with the lowest probability distance from the centroid is used to represent the cluster [36]. Three levels of wind power generation and their corresponding scenarios are illustrated in Fig. 4. Due to the different PF of loads, commonly between 0.7 and 0.9, reactive power compensation is considered in wind turbines to keep grid security especially in case of islanding.

C. Contingency Analysis

In order to analyze the benefits of introducing renewable generation and storage units in EDS, three case studies under an $N-1$ criterion are represented: 1) CA without RES and ESS; 2) CA including RES; and 3) CA including RES and ESS. This is performed by implementing a contingency parameter C_{ij} per branch to locate the fault in the network. The results are shown in terms of demand and wind curtailment cost (Table III), active power losses (Table IV), and production and storage cost (Table V).

1) Case Study 1—CA Without RES and ESS: In this case, the only power resource is the power injection from the substation to the disturbed system. Consequently, the total power losses are more than the other case studies due to the location of loads at remote nodes. Also, in some situations, a contingency leads to the isolation of the network from the substation, e.g., C_{1-2} (a contingency in the branch between nodes 1 and 2) or C_{2-3} resulting in a blackout. Regarding power losses, some selected results are shown in Table IV. For case study 1, the highest amount is related to C_{60-61} and C_{61-62}. In this case, due to the significant amount of load at node 62, which is far from the power source, power losses increase dramatically.

TABLE III
$N-1$ CONTINGENCY CURTAILMENT COST ANALYSIS ($)

Demand curtailment cost ($)							
Cont.	Case 1	Case 2			Case 3		
		Low	Mean	High	Low	Mean	High
C_{1-2}	275.75	271.15	231.75	188.47	233.66	194.5	151.34
C_{2-3}	275.75	271.15	231.75	188.47	233.66	194.5	151.34
C_{3-4}	268	266.84	248.25	226.48	248.19	227.5	205.63
C_{3-29}	29	5.30	0	0	0	0	0
C_{4-5}	5.04	0	0	0	0	0	0
C_{5-48}	2.38	0	0	0	0	0	0
C_{9-52}	3.66	3.66	3.66	3.66	3.66	3.66	3.66
C_{12-67}	2.99	2.99	2.99	2.99	2.99	2.99	2.99
C_{13-69}	4.64	4.64	4.64	4.64	4.64	4.64	4.64
C_{29-30}	5.39	3.14	0	0	0	0	0
C_{30-31}	3.24	0.98	0	0	0	0	0
C_{31-32}	3.24	0.98	0	0	0	0	0
C_{32-33}	3.24	0.98	0	0	0	0	0
C_{33-34}	3.24	0.98	0	0	0	0	0
C_{34-35}	2.10	2.10	2.10	2.10	2.10	2.10	2.10
C_{35-36}	0.48	0.48	0.48	0.48	0.48	0.48	0.48
C_{48-49}	2.38	0	0	0	0	0	0
C_{49-50}	1.64	0	0	0	0	0	0
C_{50-51}	0.58	0	0	0	0	0	0
C_{52-53}	0.30	0.30	0.30	0.30	0.30	0.30	0.30
C_{60-61}	21.7	0	0	0	0	0	0
C_{61-62}	21.7	0.22	0	0	0	0	0
C_{67-68}	1.49	1.49	1.49	1.49	1.49	1.49	1.49
C_{69-70}	2.32	2.32	2.32	2.32	2.32	2.32	2.32
Wind curtailment cost ($)							
Cont.		Case 2			Case 3		
		Low	Mean	High	Low	Mean	High
C_{3-29}		0	10.6	28.18	0	0	11.98
C_{29-30}		0	12.6	30.19	0	0	13.95
C_{30-31}		0	14.8	32.06	0	14.8	32.06
C_{31-32}		0	14.8	32.06	0	14.8	32.06
C_{32-33}		0	14.8	32.06	0	14.8	32.06
C_{33-34}		0	14.8	32.06	0	14.8	32.06

TABLE IV
$N-1$ CONTINGENCY LOSS ANALYSIS

Losses (kW)							
Cont.	Case 1	Case 2			Case 3		
		Low	Mean	High	Low	Mean	High
C_{1-2}	0	0.02	0.33	1.29	0.06	0.61	1.84
C_{2-3}	0	0.02	0.33	1.29	0.06	0.55	1.84
C_{3-4}	0.08	0.01	0.27	1.23	0.03	0.27	1.17
C_{3-29}	39.41	22.79	25.85	27.06	22.31	19.99	24.62
C_{4-5}	98.82	82.7	74.98	59.97	74.04	66.22	50.69
C_{4-37}	40.53	28.39	21.46	19.93	27.73	20.67	18.74
C_{5-6}	40.56	29.38	21.47	18.07	28.47	20.68	17.52
C_{5-48}	85.04	71.64	60.99	50.61	58.97	50.46	41.07
C_{29-30}	39.42	24.56	23.6	19.63	23.72	21.02	24.24
C_{30-31}	38.66	24.41	21.59	18.13	23.53	21.09	17.03
C_{31-32}	38.66	24.41	21.59	18.13	23.53	20.8	17.03
C_{32-33}	38.66	24.41	21.59	18.13	23.53	20.55	17.03
C_{33-34}	38.66	24.41	21.59	18.13	23.53	20.55	17.03
C_{34-35}	38.68	24.47	20.52	20.05	23.71	19.7	16.66
C_{35-36}	38.72	25.31	20.6	17.18	24.31	19.73	16.49
C_{59-60}	38.74	25.31	20.5	17.58	23.57	19.71	17.43
C_{60-61}	314.82	68.19	55.06	43.20	69.43	54.47	40.75
C_{61-62}	314.82	68.19	55.06	43.20	69.43	54.77	40.75
C_{62-63}	35.21	24.43	21.2	18.17	23.69	20.1	17.63

TABLE V
$N-1$ CONTINGENCY STORAGE COST ANALYSIS ($)

Contingency	C^{sp}	C^{rp}	$\hat{C}^{rp}$	C^{ss}	C^{rs}	$\hat{C}^{rs}$
Low level of wind						
C_{1-2}	0.0135	0	0	0	0	0
C_{2-3}	0.0135	0	0	0	0	0
C_{3-29}	0.0085	0.0003	0.0002	0	0	0
C_{29-30}	0.0077	0.0003	0.0002	0	0	0
Other branches	0.0135	0	0	0	0	0
Mean level of wind						
Contingency	C^{sp}	C^{rp}	$\hat{C}^{rp}$	C^{ss}	C^{rs}	$\hat{C}^{rs}$
C_{1-2}	0.0125	0.0024	0.0010	0	0	0
C_{2-3}	0.0124	0.0025	0.0011	0	0	0
C_{3-29}	0.0068	0	0	0.021	0.014	0.0085
C_{29-30}	0.0068	0	0	0.0154	0.0071	0.0008
Other branches	0.0135	0	0	0	0	0
High level of wind						
Contingency	C^{sp}	C^{rp}	$\hat{C}^{rp}$	C^{ss}	C^{rs}	$\hat{C}^{rs}$
C_{1-2}	0.0135	0	0	0	0	0
C_{2-3}	0.0135	0	0	0	0	0
C_{3-29}	0.0068	0	0	0.021	0.014	0.014
C_{29-30}	0.0068	0	0	0.0154	0.0071	0.0071
Other branches	0.0135	0	0	0	0	0

In addition, demand curtailment (see Table III), especially for C_{60-61} and C_{61-62}, is remarkable due to the high amount of demand at node 62 and the power flow limitation of the connection branches.

2) Case Study 2—CA Including RES: An obvious difference with respect to case study 1 is the reduction of power losses. As shown in Table IV, real power losses drop roughly 50% for most contingencies considering the mean level of wind generation. The reduction of power losses is expected due to the availability of wind power for local loads. Although the maximum power losses are relevant to contingency C_{4-5}, power losses for C_{60-61} and C_{61-62} are still remarkable. In case of contingency C_{4-5}, the main connection branch to transfer power from the substation to the remote loads is disconnected and power losses are unavoidable, however, as shown in Table III, demand curtailment is zero, in this case. Moreover, total demand curtailment is reduced in some cases, especially for contingencies C_{60-61} and C_{61-62}, due to the availability of wind power for loads at node 62.

In case of low wind generation, the amount of demand curtailment cost and power losses are similar to Case 1, as wind power generation feeds very few loads.

In addition, C_{1-2}, C_{2-3}, and C_{3-4} create an island for the whole network and, despite demand curtailment reduction under these conditions (unlike case study 1), the main part of the demand is not served yet, due to a lack of real power generation. Likewise, an island appears in case of contingency C_{3-29} for a part of the network, as shown in Fig. 3. Here, the mean level of wind generation is able to meet the demand in this area, however, wind curtailment is inevitable due to the imbalance of load and generation. Lastly, since nodes 31, 32, and 33 are not connected to any load, wind curtailment is equal for contingencies C_{30-31}, C_{31-32}, C_{32-33}, and C_{33-34}, as shown in Table III. Since the demand is constant in islanding situations ($C_{1-2}, C_{2-3}, C_{3-4}, C_{3-29}$, and C_{29-30}) by increasing the level of wind production (from a low level to higher levels), the cost of wind curtailment rises. On the other hand, with more wind power production, more loads can be fed, thus, the cost of demand curtailment drops.

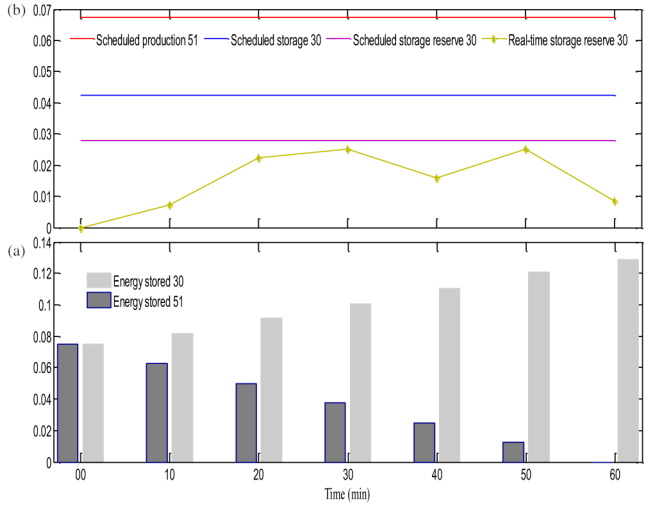

Fig. 5. Energy production/storage under a contingency in branch 3-29. (a) Energy stored (p.u.). (b) Power produced/stored (p.u.).

3) Case Study 3—CA Including RES and ESS: Using mean wind production level and compared with case study 2, ESS reduces power losses, wind and demand curtailment slightly. As illustrated in Table IV, excluding C_{1-2}, C_{2-3}, and C_{3-4}, in the other cases, power losses are reduced moderately. In spite of a fair growth of power losses for C_{1-2}, C_{2-3}, and C_{3-4} (see Table IV), the reduction of demand curtailment is noticeable, as shown in Table III. Storage units improve the operation of the network, particularly in case of islanding for the whole or a part of the network.

As shown in Table III, in cases with islanding, i.e., C_{1-2}, C_{2-3}, and C_{3-4}, the total load connected to the network is increased compare with case study 2. Likewise, for C_{3-29}, the total wind generation capacity is exploited in the presence of a storage unit in the isolated area.

In extreme situations with a high level of wind in islanding areas, as in C_{3-29} and C_{29-30}, the storage units store the extra power production to avoid demand curtailment and minimize their costs.

Since demand is higher than generation in some isolated (C_{1-2}, C_{2-3}, and C_{3-4}) areas, with a higher level of wind generation, wind and demand curtailments decrease.

As presented in Table IV, with a higher level of wind production, excluding islanding conditions, the power losses decline due to the availability of local power for loads.

Fig. 5 shows the behavior of the storage units with mean wind production in case of contingency C_{3-29}. In Fig. 5(a), the energy level of the storage units is illustrated. As C_{3-29} creates an isolated area with more generation than load, the storage unit in that section (node 30) is scheduled to store energy to avoid wind curtailment. On the other hand, the storage unit at node 51 is scheduled to produce and compensate the lack of real power.

Fig. 5(b) shows the real-time power storage of unit 30 (green line). Real-time production/storage is represented when the

TABLE VI
RECONFIGURATION ANALYSIS: OPEN SWITCHES

Cont.	Open switches	Cont.	Open switches
C_{1-2}	7-8 12-44 14-22 16-47 28-66 56-57	C_{28-66}	12-44 16-47 19-20 56-57
C_{2-3}	7-8 12-44 14-22 16-47 28-66 56-57	C_{29-30}	12-44 16-47 19-20 28-66 56-57
C_{3-4}	7-8 12-44 14-22 16-47 28-66 56-57	C_{30-31}	12-44 16-47 19-20 28-66 56-57
C_{3-29}	12-44 16-47 19-20 28-66 56-57	C_{31-32}	12-44 16-47 19-20 28-66 56-57
C_{4-5}	16-47 19-20 28-66 56-57	C_{32-33}	12-44 16-47 19-20 28-66 56-57
C_{4-37}	16-47 19-20 28-66 56-57	C_{33-34}	12-44 16-47 19-20 28-66 56-57
C_{5-6}	12-44 14-22 19-20 56-57	C_{34-35}	12-44 16-47 19-20 28-66 56-57
C_{5-48}	12-44 14-22 16-47 28-66	C_{35-36}	12-44 16-47 19-20 28-66 56-57
C_{6-7}	12-44 14-22 19-20 56-57	C_{37-38}	16-47 19-20 28-66 56-57
C_{7-8}	12-44 14-22 19-20 56-57	C_{38-39}	16-47 19-20 28-66 56-57
C_{8-9}	12-44 14-22 19-20 56-57	C_{39-40}	16-47 19-20 28-66 56-57
C_{9-10}	12-44 14-22 19-20 56-57	C_{40-41}	16-47 19-20 28-66 56-57
C_{9-52}	16-47 19-20 28-66 41-42 56-57	C_{41-42}	16-47 19-20 28-66 56-57
C_{10-11}	16-47 19-20 28-66 56-57	C_{42-43}	16-47 19-20 28-66 56-57
C_{10-54}	12-44 14-22 16-47 19-20	C_{43-44}	16-47 19-20 28-66 56-57
C_{11-12}	12-44 19-20 28-66 56-57	C_{44-45}	12-44 19-20 28-66 56-57
C_{12-13}	12-44 19-20 28-66 56-57	C_{45-46}	12-44 19-20 28-66 56-57
C_{12-44}	16-47 19-20 28-66 56-57	C_{46-47}	12-44 19-20 28-66 56-57
C_{12-67}	12-44 14-22 19-20 56-57	C_{48-49}	12-44 14-22 16-47 28-66
C_{13-14}	12-44 19-20 28-66 56-57	C_{49-50}	12-44 14-22 16-47 28-66
C_{13-69}	12-44 14-22 19-20 56-57	C_{50-51}	12-44 14-22 16-47 28-66
C_{14-15}	12-44 19-20 28-66 56-57	C_{51-60}	12-44 16-47 19-20 28-66
C_{14-22}	16-47 28-66 41-42 56-57	C_{52-53}	16-47 19-20 28-66 41-42 56-57
C_{15-16}	12-44 19-20 28-66 56-57	C_{54-55}	12-44 14-22 16-47 28-66
C_{16-17}	12-44 16-47 28-66 56-57	C_{55-56}	7-8 16-47 19-20 28-66
C_{16-47}	12-44 19-20 28-66 56-57	C_{56-57}	7-8 16-47 19-20 28-66
C_{17-18}	12-44 16-47 28-66 56-57	C_{57-58}	7-8 12-44 14-22 28-66 56-57
C_{18-19}	12-44 16-47 28-66 56-57	C_{58-59}	7-8 12-44 14-22 28-66 56-57
C_{19-20}	12-44 16-47 28-66 56-57	C_{59-60}	7-8 14-22 26-47 28-66 56-57
C_{20-21}	12-44 16-47 19-20 28-66 56-57	C_{60-61}	7-8 12-44 14-22
C_{21-22}	12-44 16-47 19-20 28-66 56-57	C_{61-62}	7-8 12-44 14-22
C_{22-23}	12-44 16-47 19-20 56-57	C_{62-63}	16-47 19-20 41-42 56-57
C_{23-24}	12-44 16-47 19-20 56-57	C_{63-64}	16-47 19-20 41-42 56-57
C_{24-25}	12-44 16-47 19-20 56-57	C_{64-65}	12-44 16-47 19-20 56-57
C_{25-26}	12-44 16-47 19-20 56-57	C_{65-66}	12-44 16-47 19-20 56-57
C_{26-27}	12-44 16-47 19-20 56-57	C_{67-68}	12-44 14-22 19-20 56-57
C_{27-28}	12-44 16-47 19-20 56-57	C_{69-70}	12-44 14-22 19-20 56-57

scheduled production/storage of energy is not sufficient to compensate the power imbalance with mean wind production of the network, as it occurs for storage unit 30.

Table V contains the costs of the storage units per contingency. The total costs of the storage units are lower than the other costs in the network and, in that regard, they are efficient. With high wind production, in C_{3-29} and C_{29-30}, the storage units in isolated areas store more in real time to avoid wind curtailment. On the other hand, with low wind power, the ESS units produce in real time to compensate the power imbalance.

D. Reconfiguration Analysis

Network reconfiguration is important to analyze to meet some goals such as reduction of power losses and isolation of faults in the EDS. In this paper, reconfiguration is carried out under contingency conditions to reach the optimal point of the optimization problem. As mentioned before, Table I shows the status of the switches in the EDS. Initially, under normal conditions, S_{12-44} (switch between nodes 12 and 44), S_{16-47}, S_{19-20}, S_{28-66}, and S_{56-57} are normally open and others are normally closed. The status of the open switches is represented for case studies 2 and 3 (for the mean value of wind) in Table VI, which is the same for both cases.

In case of contingencies C_{1-2}, C_{2-3}, and C_{3-4}, the same reconfiguration is defined by the optimization problem splitting the EDS into two radial islands, one having wind only, and the other having wind and storage. Therefore, in case of disconnection of the EDS from the external grid, the optimization problem can manage the EDS to be energized avoiding a blackout in the isolated part. Noteworthy, demand and generation curtailment is reduced by having separated radial islands in areas isolated from the substation. In order to feed loads next to the contingency and to avoid demand curtailment, the optimization problem decides to close the switches near loads. On the other hand, contingencies C_{57-58}, C_{58-59}, C_{59-60}, and C_{56-57} occur near to nodes without any connected loads and the switches in these areas remain open under any condition.

In addition, the location of both, generation and contingency, influences the RDS. For instance, S_{31-32} and S_{51-60} are always closed, as they are near to generation and storage units. Finally, reconfiguration of the EDS is not changed for contingencies in branches close to each other, as in cases L_{5-51} (feeder from nodes 5 to 51), L_{7-10}, L_{12-68}, L_{13-70}, L_{24-28}, L_{29-36}, and L_{37-44}.

TABLE VII
COMPUTATION TIME (S)

Case 1	Case 2	Case 3
793.8	9262	11071

All case studies have been solved using CPLEX 11 solver in GAMS [37]. An Intel Xeon E7-4820 computer with four processors at 2 GHz and 128 GB of RAM has been used. MATLAB [38] has been used to implement scenario reduction using K-means. Table VII illustrates the computation time of every case study assuming a mean wind power and for all the contingencies. Note that, the CPU times in Table VII correspond to the whole set of contingencies for each case, which are solved one by one. It could be possible to reduce the CPU time by analyzing the branches, which are more likely to be out of operation. The CPU time could be further reduced by considering a lower number of linearization blocks.

V. CONCLUSION

In this paper, a two-stage stochastic MILP reconfiguration model under $N-1$ contingency conditions, considering wind energy and ESS with the possibility of having isolated radial grids in distribution systems, has been investigated.

An exhaustive analysis has been done to evaluate the model and, as a result, the model has been successfully applied to a distribution network to minimize total costs. Following that, the work shows the advantages of having energy storage units and renewable energy in terms of real-time operation under contingencies in distribution networks. Consequently, the penetration of storage devices and wind generation improves the operation of the network under contingency conditions and reduces power losses and demand and generation curtailment. In addition, this method improves reliability, allows for an optimal radial reconfiguration, radial islanded operation, and the reduction of real power losses. Storage units improve the operation of the network, especially in case of islanding for the whole network or a part of it. The location of storage units is important to compensate local power, i.e., power injection to local

demand and absorption of additional power from local generation. In conclusion, the proposed model can be a valuable tool for an electrical distribution company to optimally reconfigure the system by evaluating all possible contingencies of the network using wind power and energy storage.

REFERENCES

[1] F. M. Echavarren, E. Lobato, and L. Rouco, "Contingency analysis: Feasibility identification and calculation algorithm," *IEE Proc. Gener. Transm. Distrib.*, vol. 152, no. 5, pp. 645–652, Sep. 2005.

[2] G. K. Stefopoulos, Y. Fang, G. J. Cokkinides, and A. P. S. Meliopoulos, "Advanced contingency selection methodology," in *Proc. 37th Annu. North Amer. Power Symp.*, Oct. 23–25, 2005, pp. 67–73.

[3] M. H. Sulaiman, O. Aliman, and S. R. A. Rahim, "Contingency analysis of embedded generation deployment in distribution network," in *Proc. 4th Int. Power Eng. Optim. Conf. (PEOCO)*, Jun. 23–24, 2010, pp. 412–417.

[4] A. Mendes, N. Boland, P. Guiney, and C. Riveros, "(N-1) contingency planning in radial distribution networks using genetic algorithms," in *Proc. IEEE/PES Transm. Distrib. Conf. Expo. Latin Amer. (T&D-LA)*, Nov. 8–10, 2010, pp. 290–297.

[5] S. Fliscounakis, P. Panciatici, F. Capitanescu, and L. Wehenkel, "Contingency ranking with respect to overloads in very large power systems taking into account uncertainty, preventive, and corrective actions," *IEEE Trans. Power Syst.*, vol. 28, no. 4, pp. 4909–4917, Nov. 2013.

[6] B. Liu and Y. Zhang, "Power flow algorithm and practical contingency analysis for distribution systems with distributed generation," *Eur. Trans. Elect. Power*, vol. 19, pp. 880–889, 2009.

[7] P. A. Ruiz and P. W. Sauer, "Voltage and reactive power estimation for contingency analysis using sensitivities," *IEEE Trans. Power Syst.*, vol. 22, no. 2, pp. 639–647, May 2007.

[8] F. Milano, C. Cañizares, and M. Invernizzi, "Voltage stability constrained OPF market models considering N-1 contingency criteria," *Electr. Power Syst. Res.*, vol. 74, pp. 27–36, 2005.

[9] M. F. Akorede, H. Hizam, I. Aris, and M. Z. A. Kadir, "Contingency evaluation for voltage security assessment of power systems," in *Proc. IEEE Student Conf. Res. Develop. (SCOReD)*, Nov. 16–18, 2009, pp. 345–348.

[10] P. J. M. Lacanina, A. M. Marcolini, and J. L. M. Ramos, "DCOPF contingency analysis including phase shifting transformers," in *Proc. 18th Power Syst. Comput. Conf. (PSCC'14)*, Wroclaw, Poland, Aug. 18–22, 2014, pp. 1–4.

[11] K. W. Hedman, R. P. O'Neill, E. B. Fisher, and S. S. Oren, "Optimal transmission switching with contingency analysis," *IEEE Trans. Power Syst.*, vol. 24, no. 3, pp. 1577–1586, Aug. 2009.

[12] K. W. Hedman, M. C. Ferris, R. P. O'Neill, E. B. Fisher, and S. S. Oren, "Co-optimization of generation unit commitment and transmission switching with N-1 reliability," *IEEE Trans. Power Syst.*, vol. 25, no. 2, pp. 1052–1063, May 2010.

[13] G. Ayala and A. Street, "Energy and reserve scheduling with post-contingency transmission switching," *Electr. Power Syst. Res.*, vol. 111, pp. 133–140, 2014.

[14] C. S. Chen and M. Y. Cho, "Energy loss reduction by critical switches," *IEEE Trans. Power Del.*, vol. 8, no. 3, pp. 1246–1253, Jul. 1993.

[15] A. Merlin and G. Back, "Search for minimum-loss operational spanning tree configuration for an urban power distribution system," in *Proc. 5th Power Syst. Conf.*, Cambridge, U.K., 1975, pp. 1–18.

[16] E. R. Ramos, A. G. Expósito, J. R. Santos, and F. L. Iborra, "Path-based distribution network modeling: Application to reconfiguration for loss reduction," *IEEE Trans. Power Syst.*, vol. 20, no. 2, pp. 556–564, May 2005.

[17] H. Andrei, I. Caciula, and G. Chicco, "A comprehensive assessment of the solutions of the distribution system minimum loss reconfiguration problem," in *Proc. 7th World Energy Syst. Conf.*, Romania, Europe, Jun. 30/Jul. 2, 2008, pp. 1–6.

[18] E. Romero-Ramos, J. Riquelme-Santos, and J. Reyes, "A simpler and exact mathematical model for the computation of the minimal power losses tree," *Int. J. Electr. Power Syst. Res.*, vol. 80, pp. 562–571, May 2010.

[19] S. Ching-Tzong, C. Chung-Fu, and C. Ji-Pyng, "Distribution network reconfiguration for loss reduction by ant colony search algorithm," *Int. J. Electr. Power Syst. Res.*, vol. 75, pp. 190–199, Aug. 2005.

[20] C. F. Chang, "Reconfiguration and capacitor placement for loss reduction of distribution systems by ant colony search algorithm," *IEEE Trans. Power Syst.*, vol. 23, no. 4, pp. 1747–1755, Nov. 2008.

[21] K. Prasad, R. Ranjan, N. C. Sahoo, and A. Chaturvedi, "Optimal reconfiguration of radial distribution systems using a fuzzy mutated genetic algorithm," *IEEE Trans. Power Del.*, vol. 20, no. 2, pp. 1211–1213, Apr. 2005.

[22] J. Mendoza, R. López, D. Morales, E. López, P. Dessante, and R. Moraga, "Minimal loss reconfiguration using genetic algorithms with restricted population and addressed operators: Real application," *IEEE Trans. Power Syst.*, vol. 21, no. 2, pp. 948–954, May 2006.

[23] E. Carreño, R. Romero, and A. Padilha-Feltrin, "An efficient codification to solve distribution network reconfiguration for loss reduction problem," *IEEE Trans. Power Syst.*, vol. 23, no. 4, pp. 1542–1551, Nov. 2008.

[24] P. Rezaei and M. Vakilian, "Distribution system efficiency improvement by reconfiguration and capacitor placement using a modified particle swarm optimization algorithm," in *Proc. Int. Symp. Mod. Electr. Power Syst. (MEPS)*, Sep. 20–22, 2010, pp. 1–6.

[25] R. Billinton and D. Huang, "Incorporating wind power in generating capacity reliability evaluation using different models," *IEEE Trans. Power Syst.*, vol. 26, no. 4, pp. 2509–2517, Nov. 2011.

[26] Y. M. Atwa and E. F. El-Saadany, "Optimal allocation of ESS in distribution systems with a high penetration of wind energy," *IEEE Trans. Power Syst.*, vol. 25, no. 4, pp. 1815–1822, Nov. 2010.

[27] J. M. Gantz, S. M. Amin, and A. M. Giacomoni, "Optimal mix and placement of energy storage systems in power distribution networks for reduced outage costs," in *Proc. IEEE Energy Convers. Congr. Expo. (ECCE)*, Sep. 20, 2012, vol. 15, pp. 2447–2453.

[28] D. Pozo and J. Contreras, "Unit commitment with ideal and generic energy storage units," *IEEE Trans. Power Syst.*, vol. 29, no. 6, pp. 2974–2984, Nov. 2014.

[29] B. Moradzadeh and K. Tomsovic, "Reconfiguration of a distribution system with load uncertainty," in *Proc. Int. Conf. Intell. Syst. Appl. Power Syst.*, Tokyo, Japan, Jul. 1–4. 2003, pp. 1–6.

[30] B. Moradzadeh and K. Tomsovic, "Mixed integer programming-based reconfiguration of a distribution system with battery storage," in *Proc. North Amer. Power Symp. (NAPS)*, Urbana-Champaign, IL, USA, Sep. 9–11, 2012, pp. 1–6.

[31] J. F. Franco, M. J. Rider, M. Lavorato, and R. Romero, "A mixed integer LP model for the reconfiguration of radial electric distribution systems considering distributed generation," *Electr. Power Syst. Res.*, vol. 97, pp. 51–60, Apr. 2013.

[32] H. Chiang and R. Jean-Jumeau, "Optimal network reconfigurations in distribution systems. II. Solution algorithms and numerical results," *IEEE Trans. Power Del.*, vol. 5, no. 3, pp. 1568–1574, Jul. 1990.

[33] Red Eléctrica de España. (2014). *Electricity Demand Tracking in Real-time, Associated Generation Mix and CO2 Emissions* [Online]. Available: https://demanda.ree.es/

[34] P. Pinson, G. Papaefthymiou, B. Klockl, and H. A. Nielsen, "Generation of statistical scenarios of short-term wind power production," in *Proc. IEEE Power Tech*, Lausanne, Switzerland, Jul. 1–5, 2007, pp. 491–496.

[35] K. Orwig *et al.*, "Recent trends in variable generation forecasting and its value to the power system," *IEEE Trans. Sustain. Energy*, vol. 6, no. 3, pp. 924–933, Jul. 2015.

[36] D. Arthur and S. Vassilvitskii, "K-means++: The advantages of careful seeding," in *Proc. 18th Annu. ACM-SIAM Symp. Discr. Algorithms*, New Orleans, LA, USA, 2007, pp. 1027–1035.

[37] A. Brooke, D. Kendrick, A. Meeraus, and R. Raman, *GAMS/CPLEX 9.0. User Notes*. Washington, DC, USA: GAMS Development Corp., 2003.

[38] The Mathworks Inc. (2015). *Matlab* [Online]. Available: http://www.mathworks.com

Pilar Meneses de Quevedo received the B.S. degree in industrial engineering from the University of Cantabria, Spain, in 2005, and the M.Sc. degree in the electric power industry from the Universidad Pontificia Comillas, Madrid, Spain, in 2008. She is currently pursuing the PhD. degree in electrical engineering at the University of Castilla-La Mancha, Ciudad Real, Spain.

Her research interests include power systems operations, planning, and electricity markets.

Javier Contreras (SM'05–F'15) received the B.S. degree in industrial engineering from the University of Zaragoza, Zaragoza, Spain, the M.Sc. degree in electrical engineering from the University of Southern California, Los Angeles, CA, USA, and the Ph.D. degree in electrical engineering from the University of California, Berkeley, CA, USA, in 1989, 1992, and 1997, respectively.

He is currently a Full Professor with the University of Castilla–La Mancha, Ciudad Real, Spain. His research interests include power systems planning, operations and economics, and electricity markets.

Marcos J. Rider (S'97–M'06) received the B.Sc. (Hons.) and P.E. degrees from the National University of Engineering, Lima, Perú, in 1999 and 2000, respectively, the M.Sc. degree from the Federal University of Maranhão, Maranhão, Brazil, in 2002, and the Ph.D. degree from the University of Campinas (UNICAMP), Campinas, Brazil, in 2006, all in electrical engineering.

Currently, he is a Professor with the Department of Systems and Energy, UNICAMP. His research interests include development of methodologies for the optimization, planning, and control of electrical power systems, and applications of artificial intelligence in power systems.

Javad Allahdadian received the M.Sc. degree in electrical engineering from the Universiti Teknologi Malaysia (UTM), Johor Bahru, Malaysia, in 2009, and the Ph.D. degree in electrical engineering from the Politecnico di Milano, Milano, Italy, in 2013.

Currently, he is a Researcher with the Department of Energy (DENERG), Politecnico di Torino, Turin, Italy. His research interests include power system analysis and optimization, power system dynamics and stability, and renewable energy and smart grids.